THE JOURNAL OF PHYSICAL CHEMISTRY A
A JOURNAL OF THE AMERICAN CHEMICAL SOCIETY

pubs.acs.org/JPCA

Article

Competition between Binding to Various Sites of Substituted Imidazoliums

Akhtam Amonov and Steve Scheiner*

Cite This: J. Phys. Chem. A 2023, 127, 6292−6299

Read Online

ACCESS | Metrics & More | Article Recommendations

ABSTRACT: The imidazolium cation has a number of different sites that can interact with a nucleophile. Adding a halogen atom (X) or a chalcogen (YH) group introduces the possibility of an NX···nuc halogen or NY···nuc chalcogen bond, which competes against the various H-bonds (NH and CH donors) as well as the lone pair···π interaction wherein the nucleophile lies above the plane of the cation. Substituted imidazoliums are paired with the NH_3 base, and the various different complexes are evaluated by density functional theory (DFT) calculations. The strength of XB and YB increases quickly along with the size and polarizability of the X/Y atom, and this sort of bond is the strongest for the heavier Br, I, Se, and Te atoms, followed by the NH···N H-bond, but this order reverses for Cl and S. The various CH···N H-bonds are comparable to one another and to the lone pair···π bond, all with interaction energies of 10−13 kcal/mol, values which show very little dependence upon the substituent placed on the imidazolium.

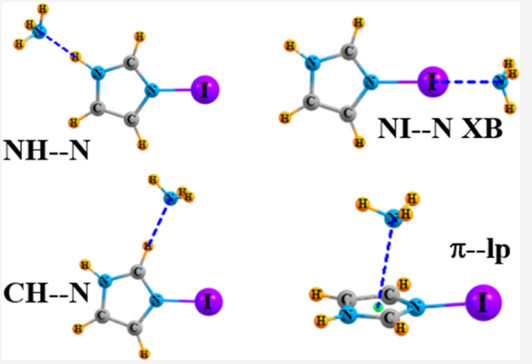

INTRODUCTION

A great deal of research over the last few years has turned to a family of noncovalent bonds that are close cousins of the venerable hydrogen bond (HB).[1−6] These interactions simply replace the bridging proton of an HB by any of a large assortment of atoms, usually but not always, more electronegative than H.[7−16] The classification system that has been developed names the bond after the column of the periodic table from which the bridging atom is drawn. Thus, a halogen bond (XB) places an atom like Cl, Br, or I in the central location, whereas S, Se, or Te refer to a chalcogen bond (YB), and so on. An initial skepticism concerning the existence of these bonds stemmed from the simple fact that the higher electronegativity of the bridging atom ought to preclude the polarity of the RH proton donor of the HB, where the partial positive charge on the H attracts the negative segment of the base. But it was soon explained[17−28] that although the overall charge of the atom, Br for instance, might be negative, there is nonetheless a small region, situated along the extension of the R−Br bond, that suffers from a depletion of electron density and is thus characterized by a positive charge. This density depletion and associated positive charge is commonly referred to as a σ-hole, which can in turn attract the negative region of the base, in much the same manner as in an HB.

The imidazole (Im) ring and its protonated imidazolium form occupy a prominent place in chemistry and biochemistry. Its presence in the His residue marks this species with particular importance in the structure and mechanism of numerous proteins and enzymes. As an example, a His residue serves as an intermediate link in the charge relay system that powers the serine proteinase family of enzymes, shuttling protons between a buried site in the protein and the residue that attacks the peptide link of a bound substrate, ultimately cleaving it.[29−33] In the realm of anion binding, a new class of highly selective anion receptors are currently being developed that utilize the Im ring as the component which directly binds the anion. In fact, the newer receptors do not use the ImH^+ imidazolium species per se but rather a cationic form, where the H is replaced by another atom; halogen, chalcogen, etc.[34−41] In the former case, the anion would be linked to ImX^+ by an NX···nuc halogen bond.[35,42]

Given its overall positive charge, an imidazolium species, or its various derivatives, can act as a potent Lewis acid by virtue not only of the NH/NX group. Each of the CH groups represents a potential proton donor in an HB to a nucleophile. One might also surmise that there will be a region of positive potential sitting directly above the plane of the Im ring, which would be a convenient hook for the lone pair of a nucleophile. These issues raise a number of important questions concerning the ability of imidazolium and its derivatives to bind to a

Received: June 17, 2023
Revised: July 12, 2023
Published: July 25, 2023

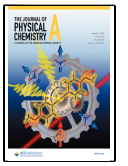

https://doi.org/10.1021/acs.jpca.3c04097
J. Phys. Chem. A 2023, 127, 6292−6299

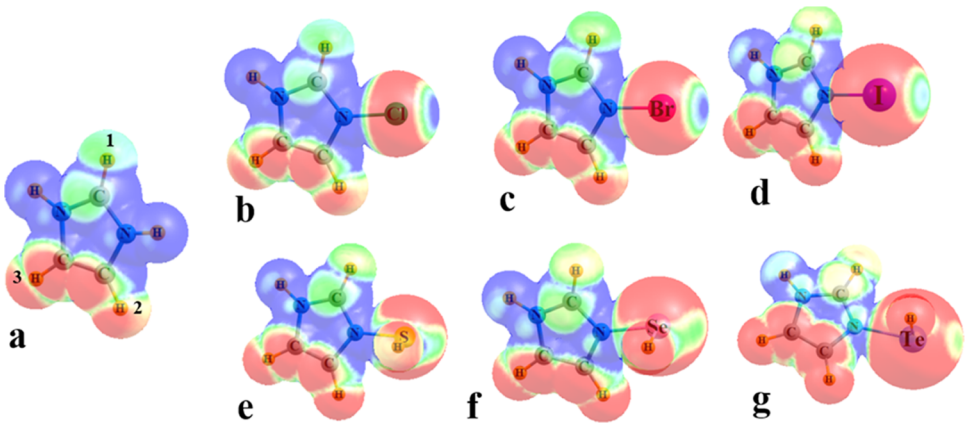

Figure 1. Molecular electrostatic potential surrounding substituted imidazolium cations: (a) ImH^+, (b–d) ImX^+, (e–g) $ImYH^+$. Blue and red colors refer to +190 and +157 kcal/mol, respectively. Numerical labels in (a) indicate CH proton designations.

Table 1. Maximum of MEP (V_{max}, kcal/mol) on ρ = 0.002 au Isodensity Surface

	H	Cl	Br	I	SH	SeH	TeH
H/X/Y	170.3	126.8	136.6	152.2	129.5	137.2	154.6
NH	170.3	172.1	172.5	165.7	168.3	165.7	161.3
CH_1	144.4	144.9	141.4	138.6	140.0	137.6	133.4
CH_2	129.2	129.8	127.3	123.9	125.1	122.4	118.5
CH_3	129.2	130.8	127.7	125.0	127.4	125.1	121.2
π	125.1	128.1	124.1	119.6	124.4	120.8	114.8
YH[a]					127.4	120.7	111.0

[a]Not along the YH axis.

nucleophile. In the first place, how does the NH···Nuc H-bond of ImH^+ stack up against the XB that might be formed by ImX^+ or the YB of $ImYH^+$. How do the two latter sorts of bonds compare with one another? How competitive are the various CH sites on each of these cationic species in terms of capturing the base? How do all of these sites compare with the π region directly above the Im ring? Another sort of possible unit is present in the chalcogen cases in the form of the proton on the Y atom of $ImYH^+$; would a YH···nuc HB be competitive with the aforementioned alternatives? As a subsidiary question, can NMR spectroscopy be applied in order to differentiate each of these sorts of binding modes from one another, and can the chemical shifts help to quantify the strength of each?

The present work applies quantum chemical calculations to address these questions. In addition to the standard ImH^+, the halogen-containing ImX^+ was examined with X = Cl, Br, and I. The chalcogen-containing $ImYH^+$ analogues were considered as well, with Y = S, Se, and Te. NH_3 was taken as the nucleophile paired with each of these Lewis acids due in part to its small size, which inhibits the formation of secondary interactions, which would blur the interpretation for each sort of desired bond. As another virtue, NH_3 is commonly used as the prototype nucleophile by several research groups, which facilitates a comparison with other calculations in the literature. The NH_3 was allowed to interact with all segments of each Lewis acid cation, thus permitting a direct comparison of binding strengths.

METHODS

Quantum chemical calculations were carried out with the aid of the Gaussian 16[43] program. The M06-2X functional[44] was applied in the context of the def2-tzvp basis set, which includes a triple-ζ foundation. This functional has been repeatedly assessed to be one of the most accurate for interactions such as those considered here.[45−52] Geometries were fully optimized and verified as true minima by the lack of any imaginary vibrational frequencies. The interaction energy E_{int} is formulated as the difference between the energy of each complex and the sum of the energies of the two subunits in the geometry they adopt within the complex. E_{int} was corrected for the basis set superposition error by the counterpoise procedure.[53] The Multiwfn program[54] located the maxima of the molecular electrostatic potential (MEP) on the ρ = 0.002 au isodensity surface of each monomer. NMR chemical shielding calculations applied the GIAO approximation.[55,56]

RESULTS

Imidazolium derivatives were constructed by placing one of several R substituents on the vacant N of $C_3N_2H_4$, leading to a species with an overall positive charge. In addition to H, which generates the classic imidazolium ion, the halogen (X) atoms Cl, Br, and I were used, as well as the SH, SeH, and TeH chalcogen (YH) groups. These cations allowed the comparison of various noncovalent bonds when combined with the universal base NH_3. With the aforementioned choice of substituents added to imidazole, each cation is capable of participating in both NH···N and CH···N H-bonds to NH_3, each of which is somewhat different due to its position within the ring. It is also possible for the base to approach the cation from directly above the ring, as a lone pair-π bond. Finally, depending on which substituent is chosen, all of the above must compete with either a halogen (X···N) or chalcogen (Y···N) bond.

Molecular Electrostatic Potentials. As a first step in understanding the various sorts of bonds, the molecular electrostatic potential (MEP) was computed for each cationic

https://doi.org/10.1021/acs.jpca.3c04097
J. Phys. Chem. A 2023, 127, 6292−6299

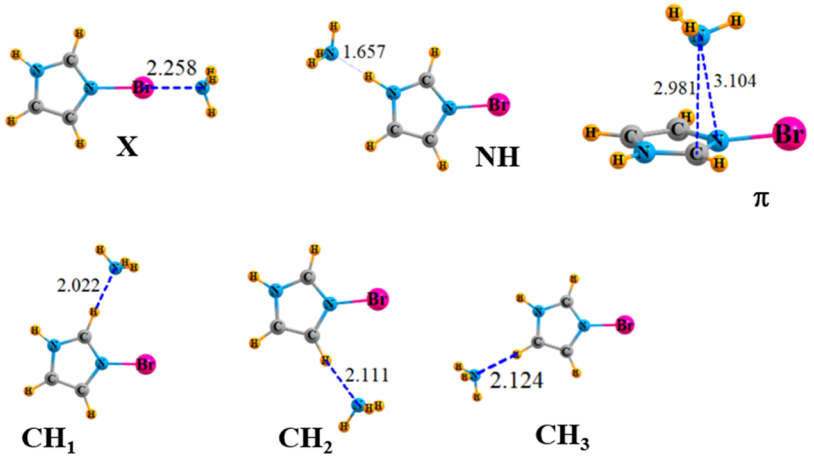

Figure 2. Geometries pairing $ImBr^+$ with NH_3. Distances in Å.

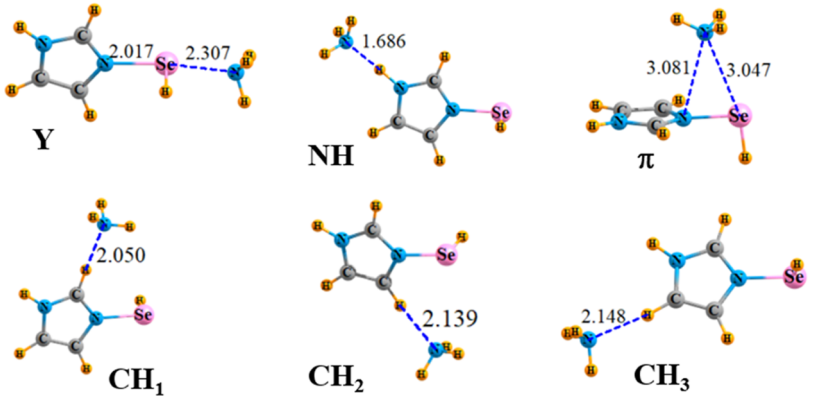

Figure 3. Geometries pairing $ImSeH^+$ with NH_3. Distances in Å.

unit. The surrounding MEP is of course quite positive, due to the overall charge of each cation. The dispositions of the MEPs are exhibited in Figure 1, where blue and red refer to the most and least positive, respectively. The NH protons of the protonated ImH^+ in Figure 1a are surrounded by the most positive (blue) MEP, followed by the CH-labeled H_1 between them, and then the other two H atoms (H_2 and H_3), which are located in red regions. This pattern is accurately reflected in the values of the associated V_{max}, corresponding to the maximum of the MEP on the ρ = 0.002 au isodensity surface, listed in the first column of Table 1. There is one additional maximum, not easily visible in Figure 1, corresponding to two symmetrically equivalent points lying above and below the molecular plane. One may think of this maximum as a π-hole, as distinguished from the other points lying along the extension of the NH and CH bonds, that fall into the σ-hole category. This point lies somewhat off of the dead center of the ring, slightly toward the C atom between the two nitrogens. The value of π V_{max} is 125.1 kcal/mol, just slightly lower than the CH σ-holes.

The MEPs of the halogenated imidazole ImX^+, where X replaces one H atom, are displayed in Figure 1b–d for X = Cl, Br, and I, respectively. With respect to the various H atoms, the pattern of ImH^+ repeats itself in that the NH occupies the bluest area, and the CH_1 between NH and NX is less positive, followed by the other two CH units. A new feature that has been added along with the X atom is the blue σ-hole lying along the extension of the N–X bond. Although the diagrams would suggest that the blue color fades in the order Cl > Br > I, the values of V_{max} on the 0.002 au isodensity surface increase in this same order, as apparent from the first row of Table 1. These halogen substitutions perturb the values of the various H atoms by only a small amount.

Another sort of substitution replaces the H of ImH^+ by a YH group where Y represents any of the chalcogen atoms S, Se, or Te. The MEPs of the resulting ImYH+ cations are presented in Figure 1e–g, all of which are quite similar to the halogenated systems above them in the figure. The σ-hole lying along the N–Y axis is indicated by the green region. Like the X series, the chalcogen holes also deepen as the Y atom grows larger and are comparable to the X holes of the corresponding row of the periodic table. The introduction of these YH groups has a small lowering effect on the various H σ-holes of some 4–5 kcal/mol. The same is true of the π-holes lying over the ring, which tend to weaken as the X or Y atom grows larger. The H atom of each YH group is also associated with a σ-hole. The values of V_{max} in the last row of Table 1 place the depth of this hole on a par with the π-hole and generally shallower than those of the other H atoms in each cation.

Interaction Energies. Inspection of the V_{max} quantities in Table 1 provides hints as to which sites might be most favorable to an interaction with a nucleophile. Figures 2 and 3 depict the optimized geometries when an NH_3 base is placed near each of the relevant σ and π-holes of the $ImBr^+$ and $ImSeH^+$ cations, respectively, as representative of the halogen- and chalcogen-substituted imidazolium. The most salient

https://doi.org/10.1021/acs.jpca.3c04097
J. Phys. Chem. A 2023, 127, 6292–6299

Table 2. Interaction Energy ($-\Delta E$, kcal/mol) of Each Site with NH_3

	H	Cl	Br	I	SH	SeH	TeH
NX/Y	22.39	18.63	28.31	33.40	19.32	25.67	31.34
NH	22.39	23.76	23.00	21.67	22.45	21.65	20.48
CH_1	13.24	13.76	13.27	12.50	12.85	12.37	11.67
CH_2	10.76	11.19	10.83	10.27	10.29	9.91	9.38
CH_3	10.76	11.15	10.83	10.33	10.61	10.30	9.82
π	9.77	10.71	10.30	9.70	10.90	10.88	12.62
YH					14.68	[a]	[a]

[a]Proton transfers to $NH_4^+ + YN_2C_3H_4$ configuration.

Table 3. Density of BCP, au

	H	Cl	Br	I	SH	SeH	TeH
H/X/Y	0.0603	0.0568	0.0720	0.0638	0.0570	0.0623	0.0553
NH	0.0603	0.0646	0.0625	0.0585	0.0605	0.0582	0.0547
CH_1	0.0258	0.0284	0.0272	0.0254	0.0266	0.0255	0.0238
CH_2	0.0213	0.0236	0.0224	0.0207	0.0217	0.0207	0.0198
CH_3	0.0213	0.0219	0.0218	0.0210	0.0210	0.0207	0.0201
π	0.0111[a]	0.0124[a]	0.0121[a]	0.0112[a]	0.0110[b]	0.0147[b]	0.0203[b]
					0.0116[c]		

[a]to C_1. [b]To Y. [c]To N.

intermolecular distances are included in these diagrams as well. The HB structures are all standard in that the NH_3 is lined up directly along the NH or CH line, with its N lone pair directed along the same axis (Searches for bifurcated H-bonds turned up no such structures as minima.). The same linearity can be said of the XB structures, and nearly so for the YB geometries as the NH_3 is only slightly displaced from the N−Y axis, a common occurrence of YBs that takes the base toward the Y σ-hole, which is also some small angle from this axis. The placement of the NH_3 within the π-complexes is interesting. As is evident in Figure 2, the N is displaced from the ring center, closer to the N that bears the X atom and the C that lies between the two N atoms of the ring. The NH_3 shifts away from the ring in the $ImYH^+$ complexes, as shown in Figure 3, finding itself above the N−Y midpoint. These shifts are sensible in that it is here that the deepest π V_{max} lies for each sort of cation.

The interaction energies of each of these complexes are reported in Table 2 and do indeed follow the general expectation of a correlation with V_{max} but with some exceptions. Either of the two NH groups of ImH^+ bind NH_3 by 22.4 kcal/mol. This quantity compares with 13.2 kcal/mol for the CH_1 lying between the two nitrogens and then 10.8 kcal/mol for the other two CH groups. Only slightly weaker is the π-hole interaction, which is just less than 10 kcal/mol, all adhering closely to the V_{max} ordering in Table 1.

The replacement of one H by X has only a small effect on these various interaction energies. They climb a small amount for $ImCl^+$ and then drop for the larger X atoms. The pattern remains the same for YH substitutions, although all of these H···N interaction energies are slightly smaller than that for X. These replacements, especially YH, raise the interaction energy with the π-hole of the cation, albeit by only a few kcal/mol at most. It is interesting to note that even though $ImTeH^+$ generates the weakest π-hole, the corresponding interaction energy is the largest for this cation. As another interesting aside, when NH_3 is aligned with the SeH or TeH proton, the latter spontaneously transfers across to it, forming an ImY···NH_4^+ pair. The SH group, on the other hand, is capable of retaining its proton, with an interaction energy of 14.7 kcal/mol, intermediate between NH and CH groups.

The greatest interest perhaps resides in the first row of Table 2, which corresponds to the halogen and chalcogen bonds of the cation with NH_3. In concert with a deepening σ-hole, E_{int} rises steeply as each sort of atom grows larger. With the exception of SH, which has a slightly larger interaction energy than Cl, the halogen bonds are somewhat stronger than the corresponding chalcogen bonds. As mentioned above, the NH group of each cation engages in the strongest H-bond with NH_3 compared to the other H atoms or the π site. It is this same H atom that engenders the deepest σ-hole. But it should be emphasized that while this NH σ-hole is uniformly deeper than that on either the X or Y atom, and by a substantial margin, it does not necessarily result in the strongest bond. The halogen bonds with both Br and I, like the Se and Te chalcogen bonds, are all stronger than the NH···N H-bond. This distinction is all the more remarkable in light of the σ-hole depths. For example, although the Br σ-hole is a full 36 kcal/mol shallower than that on the NH proton, the former forms a stronger bond with NH_3 by 5.3 kcal/mol. The bond energy difference for I is even larger, at 12 kcal/mol, despite a 13.5 kcal/mol deeper hole on NH than that on NI.

It is concluded that while the σ and π-hole depths offer some real parallels with the resulting interaction energies with a nucleophile, one must exercise caution in such predictions. Even when the σ-holes on the X and Y atoms are shallower than those on a neighboring NH, the former can punch above their weight in terms of their noncovalent bond energies. There are also reversals in the comparison of σ and π-holes wherein the latter form stronger bonds than the former, despite smaller values of V_{max}.

As a last issue, the YH substituent offers another site of interaction with a nucleophile. As may be seen in the last row of Table 2, the SH···N HB amounts to some 14.7 kcal/mol, placing it above both the CH···N HBs and the lp···π bonds. The lower electronegativity of the Se and Te atoms is such that they are unable to retain the proton, which spontaneously

https://doi.org/10.1021/acs.jpca.3c04097
J. Phys. Chem. A 2023, 127, 6292−6299

Table 4. Potential Energy Density (V, au) at BCP

	H	Cl	Br	I	SH	SeH	TeH
H/X/Y	−0.0551	−0.0457	−0.0633	−0.0593	−0.0447	−0.0542	−0.0509
NH	−0.0551	−0.0599	−0.0576	−0.0530	−0.0553	−0.0526	−0.0487
CH_1	−0.0170	−0.0195	−0.0183	−0.0167	−0.0178	−0.0168	−0.0152
CH_2	−0.0130	−0.0151	−0.0141	−0.0126	−0.0135	−0.0126	−0.0118
CH_3	−0.0130	−0.0136	−0.0135	−0.0128	−0.0129	−0.0126	−0.0121
π	−0.0066	−0.0075	−0.0073	−0.0067	−0.0073	−0.0091	−0.0129
					−0.0070		

transfers across to the nucleophile with no intervening energy barrier, yielding an $ImY\cdots HNH_3^+$ configuration.

Predictors of Energetics. It is commonly thought that some of the quantitative measures of a given AIM bond path correlate quite closely with the strength of that bond, as measured, for example, by its interaction energy. The two AIM indices that are most often cited for this purpose are the density (ρ) and the potential energy density (V) at the bond critical point. These quantities are listed in Tables 3 and 4, respectively, for each of the complexes examined here. It might be said parenthetically that the bond path for the π-complexes leads from the N of the base to different atoms of the Lewis acid. In the case of the ImH^+ and ImX^+ dimers, this path terminates on the C_1 atom lying between the two N atoms of the Im, whereas it leads to the Y atom of the $ImYH^+$ complexes (complemented by a second path to the Im N for $ImSH^+$).

There are clearly certain parallels between the energetics and AIM data. Both ρ and V correctly predict which bonding arrangement is most stable for each and every complex. For example, both ρ and V are the largest for the NH···N configuration of $ImCl^+$, but it is the NX···N XB structure that has the largest values for both Br and I. These AIM quantities also conform to the slightly most stable CH_1 as the strongest of the CH···N configurations, and only by a small margin, just as in the energetics. On the other hand, there are also areas where the AIM quantities fail to reproduce energetic trends. For example, even though I clearly engages in a stronger XB than Br, both ρ and V reverse this order; the same reversal occurs in the Se and Te YBs. The π complexes suffer from disproportionately small ρ and V. These quantities in the π-complexes are roughly half that observed in the CH···N structures, even though the energetics are quite similar.

A plot in Figure 4 of these AIM quantities against the energetics in Table 2 highlights the overall level of agreement as well as certain weaknesses. Altogether, the interaction energies in Table 2 are only roughly proportional to ρ and V, with correlation coefficients of 0.87 and 0.89, respectively. As one final point on this topic, there is some thought in the literature that the interaction energy can be roughly approximated as one-half the value of V at the bond critical point. Applying such an approximation to the data in Table 4 substantially underestimates the interaction energy, and by an inconsistent amount, by a factor varying between 1.3 and 2.6, even larger for the π-structures. It is because of the inconsistencies frequently observed between the energetics and any single AIM parameter, that the literature sometimes invokes other measures such as kinetic energy density G, ratios between V and G, density Laplacian, and total energy density H.

NMR Chemical Shifts. It has been understood for some time that the formation of an HB induces changes in the chemical shielding of not only the bridging proton but also

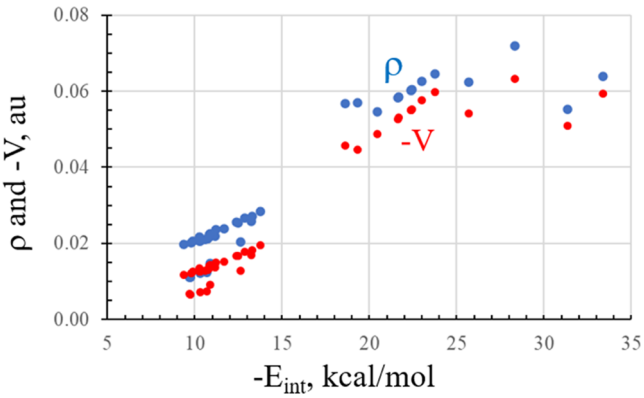

Figure 4. Relation between interaction energy and density (blue) and potential energy density (red) of the intermolecular bond critical point.

neighboring atoms such as the atom bonded to H and the electron-donating base atom. More recent work has documented evidence that the formation of other noncovalent bonds that are closely related to HBs, such as halogen and chalcogen bonds, also induces clear shifts in the NMR signal of the atoms involved.[57−64] Of this set of atoms, the one that appears to bear the closest correlation with the strength of the bond is the electron donor atom,[22,65,66] which in this case would be the N of NH_3.

The change in the isotropic chemical shielding of the basic N atom induced by the formation of each noncovalent bond is listed in Table 5, where the negative values correspond to a downfield shift. There does indeed appear to be a correlation between these shifts and the strength of the interaction, albeit an imperfect one. The most negative shielding losses, spanning the range between −29 and −39 ppm, appear in the first two rows, consistent with the strongest bonding interactions in Table 2. The NH···N HBs consistently drop the shielding by less than the XBs and YBs, though, even when the former bonds are stronger. The shielding diminutions involving the CH···N HBs are of smaller magnitude, between −10 and −15 ppm. Also, the values for CH_1 are generally more negative than those for the other two CH groups, also consonant with binding energies. The change in the N shielding when it lies above the plane of the Im ring is anomalous in some respects. For both ImH^+ and ImX^+, the base N atom suffers very little change in its shielding. However, this is not the case when the NH_3 lies above the $ImYH^+$ ring, where N loses some of its shielding, particularly for the heavier Y atoms. Indeed, $\Delta\sigma$ for the π configuration of $ImTeH^+\cdots NH_3$ is −18 ppm, larger in magnitude than any of the CH···N HB geometries.

The imperfections in the overall trend are visible in Figure 5, where there is a general correlation between the energetics and N deshielding. The four points near the bottom of the figure

https://doi.org/10.1021/acs.jpca.3c04097
J. Phys. Chem. A 2023, 127, 6292−6299

Table 5. Change in the Isotropic Shielding (ppm) of the N Atom of NH_3 Caused by Complexation

	H	Cl	Br	I	SH	SeH	TeH
H/X/Y···N	−20.8	−37.9	−39.4	−24.9	−38.6	−35.1	−23.7
NH···N	−20.8	−21.5	−21.3	−20.3	−20.6	−20.2	−19.2
CH_1···N	−13.0	−15.5	−14.8	−14.1	−14.8	−13.8	−12.9
CH_2···N	−11.1	−13.4	−12.4	−13.6	−13.5	−13.1	−13.0
CH_3···N	−11.1	−10.9	−11.4	−11.1	−10.4	−10.7	−11.0
π	−0.2	0.1	0.7	−2.1	−7.4	−10.6	−18.1

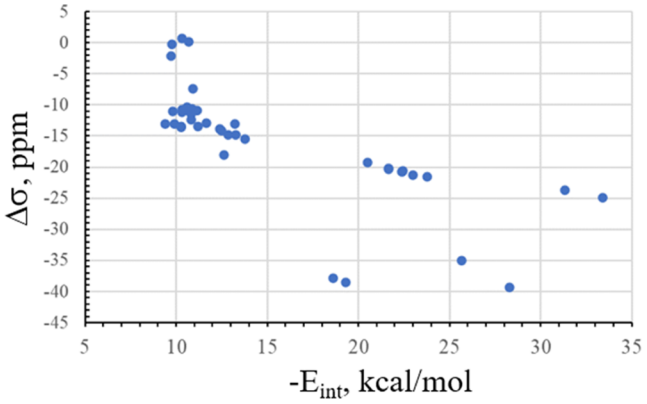

Figure 5. Relation between interaction energy and the change in the isotropic chemical shift of the N of NH_3.

with large shielding losses exceeding 35 kcal/mol refer to the XB and YB of the lighter atoms Br, I, Se, and Te. Their deviation from the points lying higher in this figure emphasizes the larger N shielding changes, out of proportion to the strength of the bonds. It may be that the proximity of these X and Y atoms is better able to adjust the magnetic properties of the N atom than the much smaller H with its single electron. The cluster of points near the top of the figure, with very small shielding changes, corresponds to the π configurations of ImH^+ and ImX^+, which exert little effect on the N. It is intriguing that the same minimal shielding change is not present in the π-complexes of the $ImYH^+$ systems. This discrepancy may be due to the specifics of the geometries. The NH_3 lies above the ring in the ImX^+ π-complexes but migrates closer to the Y atom for $ImYH^+$, as is apparent in Figures 2 and 3. The position of NH_3 above the ring enables a certain degree of shielding from the aromatic ring currents.

The exclusion of these 8 points that lie outside of the normal range leaves a solid linear relationship between E_{int} and $\Delta\sigma$, with a correlation coefficient of 0.87.

In addition to halogen-containing imidazolium cations participating in XBs, there is a good deal of literature treating similar sorts of bonds for the six-membered pyridinium systems.[67−71] The greater likelihood that a heavier X atom like Br or I will participate in an XB, as opposed to Cl, is supported by a recent survey of relevant crystal structures[72] as well as earlier work.[73−77]

CONCLUSIONS

Due in large part to its overall positive charge, the imidazolium cation and its various derivatives all engage in strong noncovalent bonds with an NH_3 nucleophile. Halogen bond strengths involving ImX^+ are comparable to chalcogen bonds of $ImYH^+$. In either set, the bond strengthens as the X or Y atom grows larger, reaching a peak exceeding 30 kcal/mol for I and Te. With the exception of the lighter Cl and S, both XB and YH are stronger than the NH···N HB of ImH^+. Another feature that the heavier atoms (Br, I, Se, and Te) have in common is that the XB/YB is the strongest bond that each cation makes with the nucleophile. The interaction with the second largest interaction energy of some 20−24 kcal/mol is the NH···N HB, followed by the various CH···N bonds, all of which are in the 9−14 kcal/mol range. The other type of interaction places the N of the base directly above the plane of the cation ring. The accompanying interaction energies are in the same range as the CH···N HBs. In many, but not all cases, the interaction energy pattern adheres to the depth of the associated maximum of the MEP surrounding the cation. One glaring exception was noted in that the σ-hole of the NH proton is uniformly deeper than that on the X or Y atom, but it is the latter that usually comprises the larger interaction energy.

AUTHOR INFORMATION

Corresponding Author

Steve Scheiner − *Department of Chemistry and Biochemistry, Utah State University, Logan, Utah 84322-0300, United States*; orcid.org/0000-0003-0793-0369; Email: steve.scheiner@usu.edu

Author

Akhtam Amonov − *Department of Optics and Spectroscopy, Engineering Physics Institute, Samarkand State University, Samarkand 140104, Uzbekistan*

Complete contact information is available at: https://pubs.acs.org/10.1021/acs.jpca.3c04097

Notes

The authors declare no competing financial interest.

ACKNOWLEDGMENTS

This material is based upon work supported by the National Science Foundation under Grant No. 1954310.

REFERENCES

(1) Joesten, M. D.; Schaad, L. J. *Hydrogen Bonding*; Marcel Dekker: New York, 1974.

(2) Desiraju, G. R.; Steiner, T. *The Weak Hydrogen Bond in Structural Chemistry and Biology*; Oxford University Press: New York, 1999.

(3) Szczesniak, M. M.; Scheiner, S. Møller-Plesset treatment of electron correlation in $(HOHOH)^-$. *J. Chem. Phys.* **1982**, *77*, 4586−4593.

(4) Cuma, M.; Scheiner, S.; Kar, T. Effect of adjoining aromatic ring upon excited state proton transfer. o-Hydroxybenzaldehyde. *J. Mol. Struct. (Theochem)* **1999**, *467*, 37−49.

(5) Gilli, G.; Gilli, P. *The Nature of the Hydrogen Bond*; Oxford University Press: Oxford, UK, 2009.

(6) Scheiner, S. *Hydrogen Bonding: A Theoretical Perspective*; Oxford University Press: New York, 1997.

(7) Gleiter, R.; Werz, D. B.; Rausch, B. J. A World Beyond Hydrogen Bonds?—Chalcogen−Chalcogen Interactions Yielding Tubular Structures. *Chem. - Eur. J.* **2003**, *9*, 2676−2683.
(8) Bleiholder, C.; Werz, D. B.; Koppel, H.; Gleiter, R. Theoretical investigations on chalcogen-chalcogen interactions: What makes these nonbonded interactions bonding? *J. Am. Chem. Soc.* **2006**, *128*, 2666−2674.
(9) Wang, W.; Ji, B.; Zhang, Y. Chalcogen bond: A sister noncovalent bond to halogen bond. *J. Phys. Chem. A* **2009**, *113*, 8132−8135.
(10) Bauzá, A.; Quiñonero, D.; Deyà, P. M.; Frontera, A. Halogen bonding versus chalcogen and pnicogen bonding: a combined Cambridge structural database and theoretical study. *CrystEngComm* **2013**, *15*, 3137−3144.
(11) Fanfrlík, J.; Přáda, A.; Padělková, Z.; Pecina, A.; Macháček, J.; Lepšík, M.; Holub, J.; Růžička, A.; Hnyk, D.; Hobza, P. The Dominant Role of Chalcogen Bonding in the Crystal Packing of 2D/3D Aromatics. *Angew. Chem., Int. Ed.* **2014**, *53*, 10139−10142.
(12) Alikhani, E.; Fuster, F.; Madebene, B.; Grabowski, S. J. Topological reaction sites − very strong chalcogen bonds. *Phys. Chem. Chem. Phys.* **2014**, *16*, 2430−2442.
(13) Trujillo, C.; Sanchez-Sanz, G.; Alkorta, I.; Elguero, J. Halogen, chalcogen and pnictogen interactions in $(XNO_2)_2$ homodimers (X = F, Cl, Br, I). *New J. Chem.* **2015**, *39*, 6791−6802.
(14) Alkorta, I.; Sánchez-Sanz, G.; Elguero, J.; Del Bene, J. E. Influence of hydrogen bonds on the P···P pnicogen bond. *J. Chem. Theory Comput.* **2012**, *8*, 2320−2327.
(15) Bauzá, A.; Quiñonero, D.; Deyà, P. M.; Frontera, A. Pnicogen−π complexes: theoretical study and biological implications. *Phys. Chem. Chem. Phys.* **2012**, *14*, 14061−14066.
(16) Galmés, B.; Juan-Bals, A.; Frontera, A.; Resnati, G. Charge-Assisted Chalcogen Bonds: CSD and DFT Analyses and Biological Implication in Glucosidase Inhibitors. *Chem. - Eur. J.* **2020**, *26*, 4599−4606.
(17) Clark, T.; Hennemann, M.; Murray, J. S.; Politzer, P. Halogen bonding: the σ-hole. *J. Mol. Model.* **2007**, *13*, 291−296.
(18) Mertsalov, D. F.; Gomila, R. M.; Zaytsev, V. P.; Grigoriev, M. S.; Nikitina, E. V.; Zubkov, F. I.; Frontera, A. On the Importance of Halogen Bonding Interactions in Two X-ray Structures Containing All Four (F, Cl, Br, I) Halogen Atoms. *Crystals* **2021**, *11*, No. 1406.
(19) Adhikari, U.; Scheiner, S. Effects of carbon chain substituent on the P···N noncovalent bond. *Chem. Phys. Lett.* **2012**, *536*, 30−33.
(20) Palusiak, M.; Grabowski, S. J. Do intramolecular halogen bonds exist? Ab initio calculations and crystal structures' evidences. *Struct. Chem.* **2008**, *19*, 5−11.
(21) Grabowski, S. J. Halogen bond and its counterparts: Bent's rule explains the formation of nonbonding interactions. *J. Phys. Chem. A* **2011**, *115*, 12340−12347.
(22) Scheiner, S.; Hunter, S. Influence of Substituents in the Benzene Ring on the Halogen Bond of Iodobenzene with Ammonia. *ChemPhysChem.* **2022**, *23*, No. e202200011.
(23) Scheiner, S. Origins and properties of the tetrel bond. *Phys. Chem. Chem. Phys.* **2021**, *23*, 5702−5717.
(24) Cunha, A. V.; Havenith, R. W. A.; van Gog, J.; De Vleeschouwer, F.; De Proft, F.; Herrebout, W. The Halogen Bond in Weakly Bonded Complexes and the Consequences for Aromaticity and Spin-Orbit Coupling. *Molecules* **2023**, *28*, No. 772.
(25) Azofra, L. M.; Scheiner, S. Tetrel, chalcogen, and CH··O hydrogen bonds in complexes pairing carbonyl-containing molecules with 1, 2, and 3 molecules of CO_2. *J. Chem. Phys.* **2015**, *142*, No. 034307.
(26) Cavallo, G.; Metrangolo, P.; Milani, R.; Pilati, T.; Priimagi, A.; Resnati, G.; Terraneo, G. The Halogen Bond. *Chem. Rev.* **2016**, *116*, 2478−2601.
(27) Scheiner, S. Sensitivity of Noncovalent Bonds to Intermolecular Separation: Hydrogen, Halogen, Chalcogen, and Pnicogen Bonds. *CrystEngComm* **2013**, *15*, 3119−3124.
(28) Taylor, A. J.; Docker, A.; Beer, P. D. Allosteric and Electrostatic Cooperativity in a Heteroditopic Halogen Bonding Receptor System. *Chem. - Asian J.* **2023**, *18*, No. e202201170.
(29) Kraut, J. Serine proteases: Structure and mechanism of catalysis. *Annu. Rev. Biochem.* **1977**, *46*, 331−358.
(30) Scheiner, S.; Kleier, D. A.; Lipscomb, W. N. Molecular orbital studies of enzyme activity: I: Charge relay system and tetrahedral intermediate in acylation of serine proteinases. *Proc. Natl. Acad. Sci. U.S.A.* **1975**, *72*, 2606−2610.
(31) Daggett, V.; Schröder, S.; Kollman, P. Catalytic pathway of serine proteases: Classical and quantum mechanical calculations. *J. Am. Chem. Soc.* **1991**, *113*, 8926−8935.
(32) Ash, E. L.; Sudmeier, J. L.; Day, R. M.; Vincent, M.; Torchilin, E. V.; Haddad, K. C.; Bradshaw, E. M.; Sanford, D. G.; Bachovchin, W. W. Unusual ^{1}H NMR chemical shifts support (His) $C^{\varepsilon 1}$-H···O═C H-bond: Proposal for reaction-driven ring flip mechanism in serine protease catalysis. *Proc. Natl. Acad. Sci., U.S.A.* **2000**, *97*, 10371−10376.
(33) Radisky, E. S.; Lee, J. M.; Lu, C.-J. K.; Koshland, D. E. Insights into the serine protease mechanism from atomic resolution structures of trypsin reaction intermediates. *Proc. Natl. Acad. Sci., U.S.A.* **2006**, *103*, 6835−6840.
(34) Walter, S. M.; Kniep, F.; Rout, L.; Schmidtchen, F. P.; Herdtweck, E.; Huber, S. M. Isothermal Calorimetric Titrations on Charge-Assisted Halogen Bonds: Role of Entropy, Counterions, Solvent, and Temperature. *J. Am. Chem. Soc.* **2012**, *134*, 8507−8512.
(35) Jungbauer, S. H.; Huber, S. M. Cationic Multidentate Halogen-Bond Donors in Halide Abstraction Organocatalysis: Catalyst Optimization by Preorganization. *J. Am. Chem. Soc.* **2015**, *137*, 12110−12120.
(36) Chakraborty, S.; Maji, S.; Ghosh, R.; Jana, R.; Datta, A.; Ghosh, P. Aryl-platform-based tetrapodal 2-iodo-imidazolium as an excellent halogen bond receptor in aqueous medium. *Chem. Commun.* **2019**, *55*, 1506−1509.
(37) Hein, R.; Beer, P. D. Halogen bonding and chalcogen bonding mediated sensing. *Chem. Sci.* **2022**, *13*, 7098−7125.
(38) Docker, A.; Guthrie, C. H.; Kuhn, H.; Beer, P. D. Modulating Chalcogen Bonding and Halogen Bonding Sigma-Hole Donor Atom Potency and Selectivity for Halide Anion Recognition. *Angew. Chem., Int. Ed.* **2021**, *60*, 21973−21978.
(39) Tse, Y. C.; Docker, A.; Zhang, Z.; Beer, P. D. Lithium halide ion-pair recognition with halogen bonding and chalcogen bonding heteroditopic macrocycles. *Chem. Commun.* **2021**, *57*, 4950−4953.
(40) Scheiner, S. Comparison of halide receptors based on H, halogen, chalcogen, pnicogen, and tetrel bonds. *Faraday Discuss.* **2017**, *203*, 213−226.
(41) Scheiner, S. Assembly of Effective Halide Receptors from Components. Comparing Hydrogen, Halogen, and Tetrel Bonds. *J. Phys. Chem. A* **2017**, *121*, 3606−3615.
(42) Bulfield, D.; Huber, S. M. Halogen Bonding in Organic Synthesis and Organocatalysis. *Chem. - Eur. J.* **2016**, *22*, 14434−14450.
(43) Frisch, M. J.; Trucks, G. W.; Schlegel, H. B.; Scuseria, G. E.; Robb, M. A.; Cheeseman, J. R.; Scalmani, G.; Barone, V.; Petersson, G. A.; Nakatsuji, H.et al. *Gaussian 16, Rev. C.01*; Wallingford, CT, 2016.
(44) Zhao, Y.; Truhlar, D. G. The M06 suite of density functionals for main group thermochemistry, thermochemical kinetics, noncovalent interactions, excited states, and transition elements: two new functionals and systematic testing of four M06-class functionals and 12 other functionals. *Theor. Chem. Acc.* **2008**, *120*, 215−241.
(45) Vamhindi, B. S. D. R.; Karton, A. Can DFT and ab initio methods adequately describe binding energies in strongly interacting C_6X_6···C_2X_n π−π complexes? *Chem. Phys.* **2017**, *493*, 12−19.
(46) Podeszwa, R.; Szalewicz, K. Density functional theory overcomes the failure of predicting intermolecular interaction energies. *J. Chem. Phys.* **2012**, *136*, No. 161102.

https://doi.org/10.1021/acs.jpca.3c04097
J. Phys. Chem. A 2023, 127, 6292−6299

(47) Karthikeyan, S.; Ramanathan, V.; Mishra, B. K. Influence of the substituents on the CH···π interaction: Benzene−methane complex. *J. Phys. Chem. A* **2013**, *117*, 6687−6694.
(48) Majumder, M.; Mishra, B. K.; Sathyamurthy, N. CH···π and π···π interaction in benzene-acetylene clusters. *Chem. Phys.* **2013**, *557*, 59−65.
(49) Vincent, M. A.; Hillier, I. H. The structure and interaction energies of the weak complexes of $CHClF_2$ and CHF_3 with HCCH: A test of denstiy functional theory methods. *Phys. Chem. Chem. Phys.* **2011**, *13*, 4388−4392.
(50) Boese, A. D. Density Functional Theory and Hydrogen Bonds: Are We There Yet? *ChemPhysChem* **2015**, *16*, 978−985.
(51) Walker, M.; Harvey, A. J. A.; Sen, A.; Dessent, C. E. H. Performance of M06, M06-2X, and M06-HF Density Functionals for Conformationally Flexible Anionic Clusters: M06 Functionals Perform Better than B3LYP for a Model System with Dispersion and Ionic Hydrogen-Bonding Interactions. *J. Phys. Chem. A* **2013**, *117*, 12590−12600.
(52) Molnar, L. F.; He, X.; Wang, B.; Merz, K. M. Further analysis and comparative study of intermolecular interactions using dimers from the S22 database. *J. Chem. Phys.* **2009**, *131*, No. 065102.
(53) Boys, S. F.; Bernardi, F. The calculation of small molecular interactions by the differences of separate total energies. Some procedures with reduced errors. *Mol. Phys.* **1970**, *19*, 553−566.
(54) Lu, T.; Chen, F. Multiwfn: A multifunctional wavefunction analyzer. *J. Comput. Chem.* **2012**, *33*, 580−592.
(55) Ditchfield, R. GIAO studies of magnetic shielding in FHF^- and HF. *Chem. Phys. Lett.* **1976**, *40*, 53−56.
(56) Alkorta, I.; Elguero, J. Ab initio (GIAO) calculations of absolute nuclear shieldings for representative compounds containing $^{1(2)}H$, $^{6(7)}Li$, ^{11}B, ^{13}C, $^{14(15)}N$, ^{17}O, ^{19}F, ^{29}Si, ^{31}P, ^{33}S, and ^{35}Cl nuclei. *Struct. Chem.* **1998**, *9*, 187−202.
(57) Southern, S. A.; Nag, T.; Kumar, V.; Triglav, M.; Levin, K.; Bryce, D. L. NMR Response of the Tetrel Bond Donor. *J. Phys. Chem. C* **2022**, *126*, 851−865.
(58) Weiss, R.; Aubert, E.; Pale, P.; Mamane, V. Chalcogen-Bonding Catalysis with Telluronium Cations. *Angew. Chem., Int. Ed.* **2021**, *60*, 19281−19286.
(59) Mikherdov, A. S.; Jin, M.; Ito, H. Exploring Au(i) involving halogen bonding with N-heterocyclic carbene Au(i) aryl complexes in crystalline media. *Chem. Sci.* **2023**, *14*, 4485−4494.
(60) Kumar, S.; Body, C.; Leyssens, T.; Van Hecke, K.; Berger, G.; Van der Lee, A.; Laurencin, D.; Richeter, S.; Clément, S.; Meyer, F. Halogen-Bonded Thiophene Derivatives Prepared by Solution and/or Mechanochemical Synthesis. Evidence of N···S Chalcogen Bonds in Homo- and Cocrystals. *Cryst. Growth Des.* **2023**, *23*, 2442−2454.
(61) Pale, P.; Mamane, V. Chalcogen Bonds: How to Characterize Them in Solution? *ChemPhysChem* **2023**, *24*, No. e202200481.
(62) Nag, T.; Ovens, J. S.; Bryce, D. L. 77Se and 125Te solid-state NMR and X-ray diffraction structural study of chalcogen-bonded 3,4-dicyano-1,2,5-chalcogenodiazole cocrystals. *Acta Crystallogr., Sect. C: Struct. Chem.* **2022**, *78*, 517−523.
(63) Scheiner, S. Characterization of Type I and II Interactions between Halogen Atoms. *Cryst. Growth Des.* **2022**, *22*, 2692−2702.
(64) Lu, J.; Scheiner, S. Relationships between Bond Strength and Spectroscopic Quantities in H-Bonds and Related Halogen, Chalcogen, and Pnicogen Bonds. *J. Phys. Chem. A* **2020**, *124*, 7716−7725.
(65) Lapp, J.; Scheiner, S. Proximity Effects of Substituents on Halogen Bond Strength. *J. Phys. Chem. A* **2021**, *125*, 5069−5077.
(66) Michalczyk, M.; Zierkiewicz, W.; Wysokiński, R.; Scheiner, S. Theoretical Studies of IR and NMR Spectral Changes Induced by Sigma-Hole Hydrogen, Halogen, Chalcogen, Pnicogen, and Tetrel Bonds in a Model Protein Environment. *Molecules* **2019**, *24*, No. 3329.
(67) Aubert, E.; Espinosa, E.; Nicolas, I.; Jeannin, O.; Fourmigué, M. Toward a reverse hierarchy of halogen bonding between bromine and iodine. *Faraday Discuss.* **2017**, *203*, 389−406.
(68) Logothetis, T. A.; Meyer, F.; Metrangolo, P.; Pilati, T.; Resnati, G. Crystal engineering of brominated tectons: N-methyl-3,5-dibromopyridinium iodide gives particularly short C−Br···I halogen bonding. *New J. Chem.* **2004**, *28*, 760−763.
(69) Fotović, L.; Stilinović, V. Halogenide anions as halogen and hydrogen bond acceptors in iodopyridinium halogenides. *CrystEngComm* **2020**, *22*, 4039−4046.
(70) Lohrman, J. A.; Deng, C.-L.; Shear, T. A.; Zakharov, L. N.; Haley, M. M.; Johnson, D. W. Methanesulfonyl-polarized halogen bonding enables strong halide recognition in an arylethynyl anion receptor. *Chem. Commun.* **2019**, *55*, 1919−1922.
(71) Riel, A. M. S.; Decato, D. A.; Sun, J.; Massena, C. J.; Jessop, M. J.; Berryman, O. B. The intramolecular hydrogen bonded−halogen bond: a new strategy for preorganization and enhanced binding. *Chem. Sci.* **2018**, *9*, 5828−5836.
(72) Fotović, L.; Bedeković, N.; Stilinović, V. Evaluation of Halogenopyridinium Cations as Halogen Bond Donors. *Cryst. Growth Des.* **2021**, *21*, 6889−6901.
(73) Awwadi, F. F.; Willett, R. D.; Peterson, K. A.; Twamley, B. The Nature of Halogen···Halide Synthons: Theoretical and Crystallographic Studies. *J. Phys. Chem. A* **2007**, *111*, 2319−2328.
(74) Freytag, M.; Jones, P. G.; Ahrens, B.; Fischer, A. K. Hydrogen bonding and halogen−halogen interactions in 4-halopyridinium halides. *New J. Chem.* **1999**, *23*, 1137−1139.
(75) Espallargas, G. M.; Zordan, F.; Arroyo Marín, L.; Adams, H.; Shankland, K.; van de Streek, J.; Brammer, L. Rational Modification of the Hierarchy of Intermolecular Interactions in Molecular Crystal Structures by Using Tunable Halogen Bonds. *Chem. - Eur. J.* **2009**, *15*, 7554−7568.
(76) Espallargas, G. M.; Brammer, L.; Sherwood, P. Designing Intermolecular Interactions between Halogenated Peripheries of Inorganic and Organic Molecules: Electrostatically Directed M-X··· X′-C Halogen Bonds. *Angew. Chem., Int. Ed.* **2006**, *45*, 435−440.
(77) Zordan, F.; Purver, S. L.; Adams, H.; Brammer, L. Halometallate and halide ions: nucleophiles in competition for hydrogen bond and halogen bond formation in halopyridinium salts of mixed halide−halometallate anions. *CrystEngComm* **2005**, *7*, 350−354.

https://doi.org/10.1021/acs.jpca.3c04097
J. Phys. Chem. A 2023, 127, 6292−6299